I CIMMEC
1ST INTERNATIONAL CONGRESS ON MECHANICAL METROLOGY
October, 08 – 10, 2008, Rio de Janeiro, Brazil

CURRENT PTB DEVELOPMENTS AND INVESTIGATIONS OF CRYSTALLINE FORCE SENSORS USED AS LOAD CELLS

Oliver Mack [1], *Sascha Mäuselein* [2]

[1] Physikalisch-Technische Bundesanstalt, Braunschweig, Germany, Oliver.Mack@ptb.de
[2] Physikalisch-Technische Bundesanstalt, Braunschweig, Germany, Sascha.Maeuselein@ptb.de

Abstract: This paper presents metrological investigations of load cells (LCs) using crystalline materials as sensor material. Particularly in combination with mechatronic systems crystalline materials afford a couple of advantages. The material behaviour is characterized by means of material constants and due to a high purity and the crystalline structure of the material ideal elastic properties and nearly no mechanical after effects are expected.

In recent years two diversity sensor systems for load cells with crystalline materials are focus of investigations at the Physikalisch-Technische Bundesanstalt (PTB). Conventional piezoelectric force transducer (PF) with quartz plates as active sensor elements leads to the assumption that static measurements of high-accuracy are not possible [1,2].

Investigations on load cells with mechanical springs made of single-crystalline silicon and sputtered-on thin film strain gauges (SGs) show mechanical after effects about a factor of 100 lower in comparison to conventional metallic load cell materials [3].

Experimental and theoretical investigations point out that both sensor systems allow high precision measurement by means of mechatronic compensation systems.

Keywords: load cell, crystalline material, piezoelectric effect, sputter-on technique, strain gauge

1. INTRODUCTION

By means of mechatronic systems environmental influence factors such as temperature and humidity – but also non-linearity – can be compensated in principal. For a useful compensation these influencing factors have to be known very well and the reproducibility of the measurement signal has to be very high. However, the compensation of time-depending effects, such as creep and hysteresis, is very difficult up to now. Firstly the characterisation of time-depending effects is very complicated due to their dependence on other factors such as temperature and humidity. Secondly the models for time-depending compensation which have to consider the whole load history of the sensor are very complex.

In opposite to metallic materials crystalline materials have a defined atomic structure. The material properties of these materials are characterised by constants and are widely independent of thermal and mechanical pretreatment of the material. Synthetic crystal growth procedures (e.g. the floating-zone procedure) allow crystalline materials to be manufactured with very high purity [4]. Due to these properties crystalline materials seems to be very suitable for mechatronic systems.

But the limits of classification of crystalline force sensors according to international recommendations like OIML R60 for LCs used in legal metrology [5] are unknown up to now. For this reason two diversity sensor systems with crystalline materials – piezoelectric force transducer and silicon (Si) load cells with sputtered-on strain gauges - are focus of investigations at PTB. First results of the investigations are discussed in this paper.

2. OIML-RECOMMENDATION R60 FOR LOAD CELLS

The OIML recommendation R60 specifies the static metrological characteristics and static evaluation procedures for LCs and considers their reproducibility, linearity, hysteresis and creep effects, as well as zero point return at 20°C, 40°C and -10°C [5]. The test sequence for each test temperature is shown in Fig. 1.

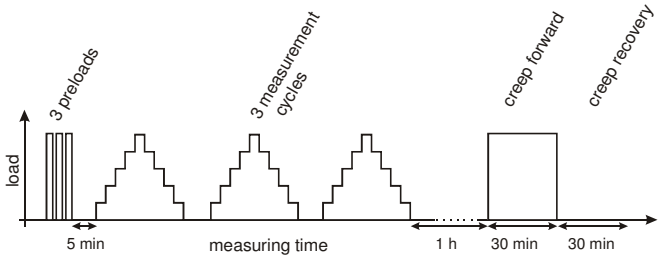

Fig. 1. Recommended test sequence for each temperature according to OIML R60

The recommendation approves of so-called accuracy tests with increasing and decreasing discrete load steps. The measurement values are taken at time intervals between 10 seconds and 60 seconds after the initiation of loading or unloading and depend on the load change. The creep forward and the creep recovery are measured for 30 minutes, respectively, and one hour after the accuracy test.

Load cells are classified in four accuracy classes, A to D, for use in special-, high-, medium- or ordinary-accuracy weighing instruments. The requirements of an accuracy class are fulfilled, if the error of measurement lies within a maximum permissible error (*mpe*). The *mpe* depends on the maximum load m and a maximum number of load cell verification intervals n_{max}. Table 1 shows the accuracy classes and the corresponding *mpe* with a verification interval

$$v = \frac{m}{n_{max}} \tag{1}$$

Table 1. Accuracy classes and the corresponding maximum permissible errors (*mpe*) according to the OIML recommendation R60. The apportionment factor is typically p_{LC}=0.7 for load cells.

mpe	class A	class B	class C	class D
$p_{LC}\times 0.5v$	$m \le 50000v$	$m \le 5000v$	$m \le 500v$	$m \le 50v$
$p_{LC}\times 1.0v$	$m \le 200000v$	$m \le 20000v$	$m \le 2000v$	$m \le 200v$
$p_{LC}\times 1.5v$	$200000v < m$	$m \le 100000v$	$m \le 10000v$	$m \le 1000v$

Subsequently not the mass m, but the force F acting on a piezoelectric force transducer, is taken into account. The force F is the product of the mass m and the local acceleration of gravity g_{loc}. Influences of humidity and barometric pressure, which are also considered in the OIML recommendation R60, are not the subject of this article.

3. PIEZOELECTRIC FORCE TRANSDUCER

Due to their small dimensions and high stiffness, piezoelectric force transducers are predestined for dynamic force measurements as impact force measurements in crash tests, for example [6,7]. Different types of these transducers with nominal loads between 5 kN and 20 kN are shown in Fig. 2.

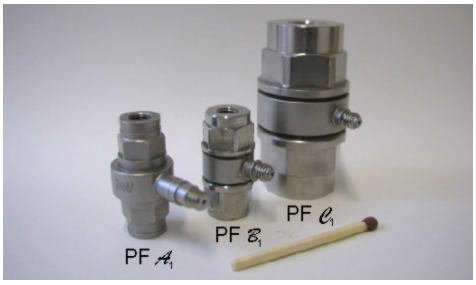

Fig. 2: Different types of PFs with nominal loads between 5 kN (PF $\mathcal{B}_1$) and 20 kN (PF $\mathcal{A}_1$ and $\mathcal{C}_1$)

A very useful type of a piezoelectric force transducer is the so-called load washer (Fig. 3).

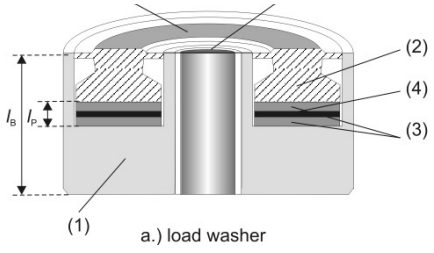

Fig 3: Schematic representation of a piezoelectric load washer

A load washer is based on a ring-shaped base plate (1) and a top plate (2), two ring-shaped quartz plates electrically connected in parallel (3), so-called x-cut plates made of α-quartz as piezoelectric sensor material and an electrode placed between the two quartz plates (4).

Load-washer-type force transducers which are already mounted and preloaded by means of two steels nuts and a preloading bolt are known as force links (Fig. 4) and permit compression and tension force measurements. The measurement range of force links is less than ± 1 kN up to over ± 100 kN [7]. Load washers enable compression force measurements even up to over 1 MN [9].

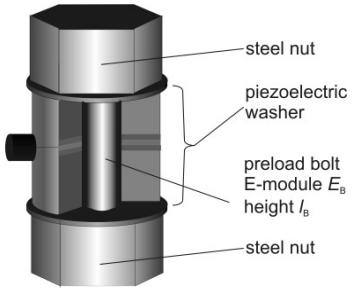

Fig 4: Schematic representation of a piezoelectric force link

The sensitivity S_{FT} determined by an analytical model described in [8] depends on the geometry and the material properties of the force link and is given by

$$S_{FT} = \frac{Q}{F} = \frac{d_{11}}{\phi + 1} \tag{2}$$

with the induced charge Q, a force shunt factor ϕ and the piezoelectric coefficient d_{11}, a material constant which is 2,3 pC/N for α-quartz.

Although PFs show a good dynamic behaviour, static sensor qualities such as linearity, hysteresis, sensitivity, reproducibility and effects of mechanical disturbance properties which are necessary for precision measurements are widely unknown [10,5]. This is due to their active measuring principle - the mechanical energy resulting from forces acting on the PF is directly transformed into electrical energy in the form of induced charges [11,12]. As a result of finite insulation resistance, the induced charges show an exponential decrease. Static high-precision measurements are not possible in principle [8].

3.1. The piezoelectric force measurement chain

To measure the induced charge Q, inverting DC amplifiers with a highly insulating range capacitor as capacitive feedback, so-called charge amplifiers, are used [8]. The capacitive feedback works like an integrator for electric charges induced by load changes acting on the force link. Due to a finite insulating resistance R_G, the range capacitor has an exponential discharge characterized by a time constant τ_G. In addition, a linear drift current I_D, caused by leakage currents of the electronic components in the input circuit of the charge amplifier and offset voltages of

the DC amplifier, affects the measurement. Furthermore, influences of cables, connectors and memory effects of force links may cause a strong and non-reproducible drift rate. With a sensitivity S_{CA} of the charge amplifier the time-dependent output voltage $U_A(t)$ due to a static force F is given by

$$U_A(t) = \left(S_{CA} \cdot S_{FT} \cdot F + I_D \cdot S_{CA} \cdot t\right) \cdot e^{-\frac{t}{\tau_G}} \qquad (3)$$

and shows that static force measurements with piezoelectric devices are not possible for long-term intervals [8,13].

By the means of insulating resistances $R_G \geq 10^{14}\ \Omega$ and capacities $C_G \approx 100$ nF of the range capacitor, special charge amplifiers reach time constants up to $\tau_G \approx 10^7$ s. This corresponds to a relative change of the measurement signal of $6 \cdot 10^{-6}$ within 60 seconds, and less than 0.02 % within 30 minutes. In this case the drift behaviour is characterised by a linear drift current I_D smaller than 0.03 pA for specially modified low-drift charge amplifiers [8]. In conjunction with these amplifiers, static force and weighing measurements are possible for piezoelectric force measuring devices if the measuring times and the times of load change are in the range of a few minutes [6, 13].

The complete piezoelectric force measuring chain is shown in the schematic drawing in Fig. 5.

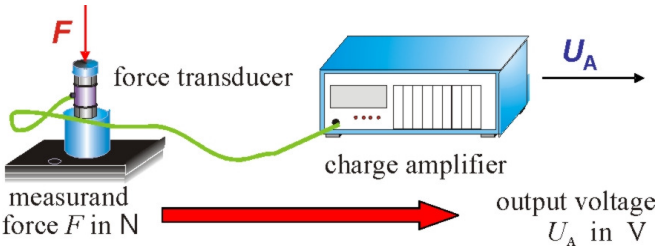

Fig. 5: Schematic drawing of a piezoelectric force measuring chain with a PF as force sensor and a charge amplifier to measure the induced charge

Based on the assumption that creep-forward and creep-recovery measurements are the crucial criterion for classification according to OIML R60, the theoretically determined n_{max} is given by

$$n_{max} = \frac{S_{FT} \cdot F \cdot mpe}{I_D \cdot t_D} . \qquad (4)$$

For a drift current $I_D = 0.03$ pA and a creeping time $t_D = 30$ min piezoelectric force measurement devices reach class D0.27 for force links with a nominal load of 5 kN. However, the theoretically attainable accuracy class increases with increasing load. Force links with nominal loads of 20 kN reach class C0.7 with 700 verification intervals, and force links with a nominal load of 100 kN reach the accuracy class C5.4 of high-precision strain gauge load cells. By still larger loads, e.g. of 200 kN, even the accuracy class C10 becomes theoretically possible, which is impossible to achieve with strain gauge load cells. Investigations of force links with nominal loads of 5 kN and 20 kN reach respectively class D0.3 and C0.8. and confirm these results.

3.2. *Experimental setup*

The accuracy tests of the force links and the subsequent drift measurements had been carried out at PTB's 5 t (50 kN) dead-load force standard machine shown in Fig. 6.

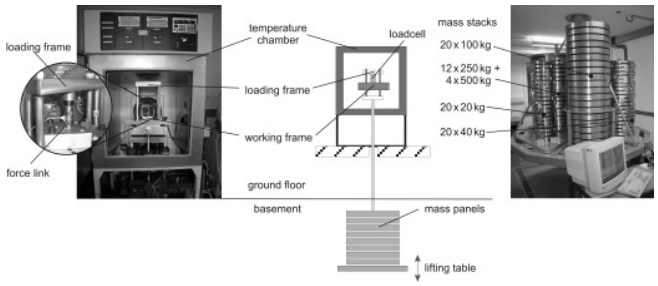

Fig. 6: 5 t (50 kN) dead-load force standard machine for the testing of load cells

The force link which will be examined is mounted on a working table. Via a loading frame, one out of a total of four mass stacks with maximum weights between 400 kg and 5 t is coupled to the force link. A lifting table allows positioning of the mass stacks and the coupling of single mass panels. For examinations in a temperature range between -10°C and +40°C, the working table, the test sample and the loading frame are accommodated inside a climatic chamber. The following investigations are carried out exemplarily with a 5 kN force link.

3.3. *Results of accuracy tests*

Figure 7 shows the characteristic curves of a 5 kN force link under -10°C, 20°C and 40°C conditions as a function of the relative load.

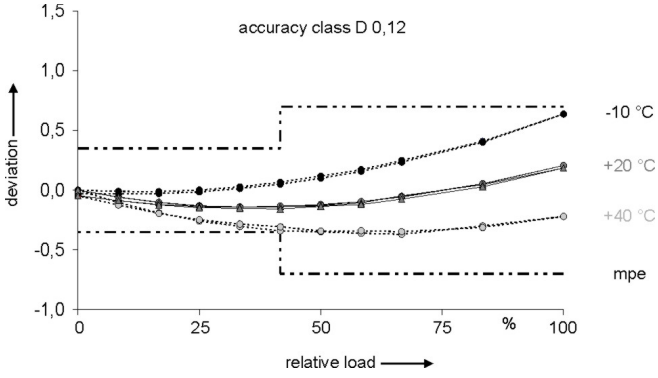

Fig. 7: Deviation expressed in verification intervals v as a function of the relative load of a 5 kN force link under -10°C, 20°C and 40°C conditions

Due to strong temperature dependencies and nonlinearities, the 5 kN force link only reaches the low class D0.12 of ordinary-accuracy weighing instruments with 120 verification intervals. The investigations point out a very

small hysteresis of the characteristic curves and in addition the influence of the drift of the charge amplifier is negligible for this accuracy class.

Consequently, not the drift or hysteresis but nonlinearities and temperature effects are the crucial criterion for the classification of the 5 kN force link.

3.4. Nonlinearity and temperature effects

Below, the material properties of the α-quartz plates used in load washers (s. Fig. 3) will be discussed in detail. By means of hydrothermal synthesis, α-quartz is produced synthetically and with high purity [7, 13]. Beyond this, α-quartz was one of the first crystals in which nonlinearities were discovered [13]. For piezoelectric force measurement the electroelastic effect – examined in detail in the 4th quarter of the last century [14] – is of particular importance but has been widely neglected up to now. The effect describing the electroelastic coefficient of x-cut quartz plates is the material constant $g_{111} = 62.3 \cdot 10^{-23}\ \mathrm{Cm^2N^{-2}}$ which specifies the quadratic relationship between mechanical stress and induced charge [7, 13].

Taking this effect into account, the nonlinear behaviour of a piezoelectric force link is given by

$$S_{FT}\left(\mathrm{d}\sigma_F, \sigma_V\right) = \frac{d_{11}}{\phi + 1} + \frac{g_{111}}{\phi + 1} \cdot \left(2\sigma_V + \mathrm{d}\sigma_F\right) \qquad (5)$$

whereby $\mathrm{d}\sigma_F$ quantifies the change of mechanical stress due to a force F acting on the force link, and σ_V describes the preload through the preloading bolt. In practice, a generally accepted conservative limit for the preload of quartz is $\sigma_{max} = 150 \cdot 10^6\ \mathrm{Nm^{-2}}$ [7]. Assuming identical ranges of compression and tension force, the maximum change of mechanical stress $\mathrm{d}\sigma_P = 75 \cdot 10^6\ \mathrm{Nm^{-2}}$ is realised with a preload of $\sigma_V = 75 \cdot 10^6\ \mathrm{Nm^{-2}}$. Additionally, temperature dependencies are taken into account by

$$d_{11}(\vartheta) = d_{11} \cdot \left(1 + \tau_{11} \cdot (\vartheta - \vartheta_0)\right) \qquad (6)$$

with a temperature coefficient $\tau_{11} = -2.15 \cdot 10^{-4}\ \mathrm{K^{-1}}$ of the coefficient d_{11} based on $\vartheta_0 = 20°\mathrm{C}$ [13]. Figure 8 pictures the characteristic curves according to eq. (5) and eq. (6) under -10°C, 20°C and +40°C conditions as a function of the relative load and based on the nominal load.

Striking is the high correlation to the characteristic curves determined experimentally (Figure 7). As a result, the investigations confirmed that the material properties are the ultimate cause of the temperature dependency and nonlinear behaviour of piezoelectric force links.

Much more of interest is the conclusion that, independent of the nominal load, all force links have in principle the same characteristic curves because their behaviour is traceable to material constants.

This means that only for small nominal load of a force link, the unknown and hardly predictable linear drift behaviour of the charge amplifier is the crucial criterion for the classification according to the OIML recommendation R60. With increasing nominal load the nonlinear and temperature behaviour become increasingly important for the classification.

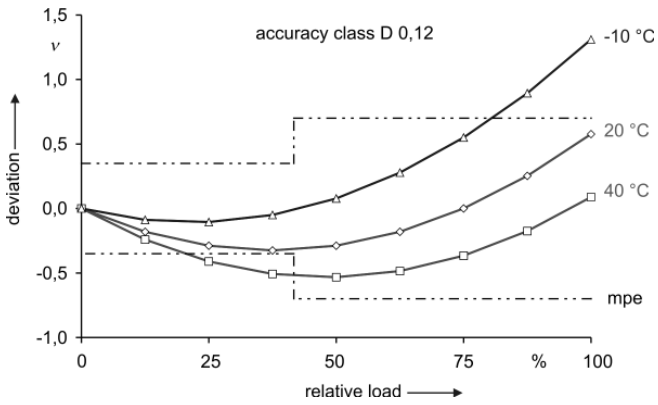

Fig. 8: Deviation expressed in verification intervals ν as a function of the relative load of analytically determined characteristic curves of piezoelectric force links under -10°C, 20°C and +40°C conditions

Due to the constant and well known material properties of α-quartz this material should be predestinated for compensating nonlinearities and temperature effects by means of mechatronic systems e.g. known from digital load cells. But for piezoelectric force measurement devices comparable systems are unknown up to now. The investigations point out especially for high-nominal loads and in conjunction with low-drift charge amplifiers, piezoelectric force measurement devices seem to offer high unused potential also for static precision measurements if suitable mechatronic systems are used.

4. SILICON LOAD CELLS WITH SPUTTERED-ON STRAIN GAUGES

Subsequent investigations at PTB concerning LCs made of single-crystalline silicon as spring material and sputtered-on strain gauges (Si-LCs) are discussed.

The manufacturing of single-crystalline Si is carried out in high purities by crystal growth processes. For this reason, silicon deforms purely elastically, shows no material fatigue, and the mechanical after-effects are negligible in comparison to metallic materials [4]. Because of these properties, single-crystalline Si seems to be predestined to be used for construction of mechanical springs of load cells.

The application of strain gauges by means of the sputtering technique leads to a direct connection between mechanical spring and SG. Sputtered-on SGs show therefore – compared to the conventional glue connections of foil strain gauges – only negligible strain-gauge creep effects. For compensating mechanical after-effects of conventional metallic materials, this may be a disadvantage, but in combination with single-crystalline silicon as material of mechanical springs, sputtered-on metal strain gauges are expected to show a high reproducibility and a low time-dependency of the measurement signal. This is because both the mechanical after-effects of single-crystalline Si as well as the creep of the SGs are low compared to metallic springs with glued foil SGs.

The mechanical spring (S-Spring) of a Si-LC is designed as double-bending beam. Next to the well known advantages of this geometry aspects of manufacturing caused by the processing of Si and the application of thin film strain gauges by the sputtering technology are mainly deciding. The nominal load of the Si-LC shown in Fig. 9 amounts 6 kg.

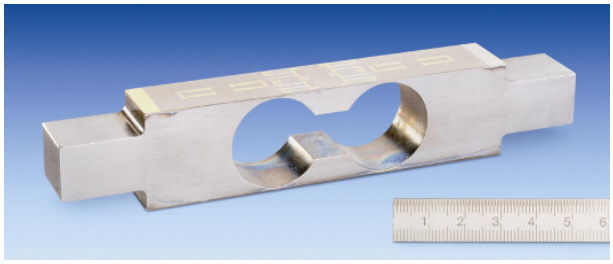

Fig. 9: **Load cell made of single crystalline silicon and sputtered on strain gauges for loads up to 6 kg**

In the following sections two measurement results are presented. The mechanical after effects of the S-Spring without SGs are determined by load depending deformation measurements. Comparative investigations of Si- and metallic LCs of the same geometry according to OIML R60 are presented in the ensuing section for a temperature of 20°C.

4.1. Mechanical aftereffects of the silicon spring

To perform experimental deformation measurements at a temperature of 20 °C on the S-Spring a Fizeau interferometer available at PTB is used. This interferometer delivers position depending height information data of a surface topology within a short time interval [3].

The schematically arrangement of the experimental setup with the Fizeau interferometer and a S-Spring as device under test is shown in figure 10.

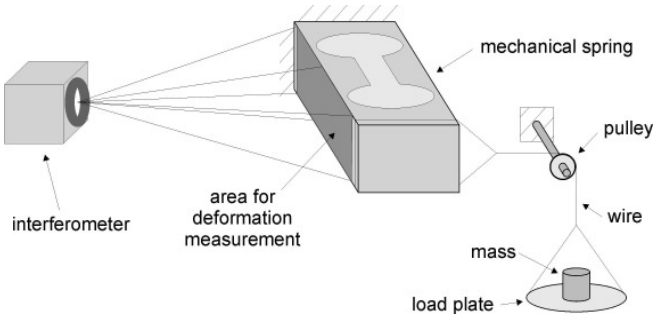

Fig. 10: Schematic arrangement of the experimental setup to measure the deformation of a mechanical spring under load

Unfortunately the Fizeau interferometer is fix mounted on a vibration isolated table and has a horizontal path of rays. This requires a mounting of the S-Spring rotated by 90 degrees as shown in figure 10 to achieve a perpendicular alignment between the surface of the LC and the laser beams.

This requires a force introduction to the S-Spring by putting weights on a load plate and switching the weight force via a wire and a pulley with low friction in horizontal direction.

By analysing the 3-D topology data of the surface in a suitable way as described in [3] the deformation measurements become independent from drift effects of the experimental setup. Elongations of the experimental setup can be eliminated as well as the tipping of the S-Spring within the experimental setup. The elimination of these influencing factors is very important, especially for time-dependent measurements as the measurement of mechanical after effects. The analytical compensation of the deflection error caused by tipping of the S-Spring allows the evaluation of the mechanical after effect with the required accuracy [3].

To investigate the mechanical after effects the nominal load is applied for 30 minutes (loading) and then all masses and the load plate are removed for 30 minutes (unloading).

The first creep measurement is performed with a nominal load of 400 g. This load leads to the maximum deflection detectable by the interferometer. To achieve higher absolute measurement values for the time depending deflection a second creep measurement is taken out with a nominal load of 3000 g. For this measurement while loading no deflection could be measured due to the limit of the measurement range of the interferometer.

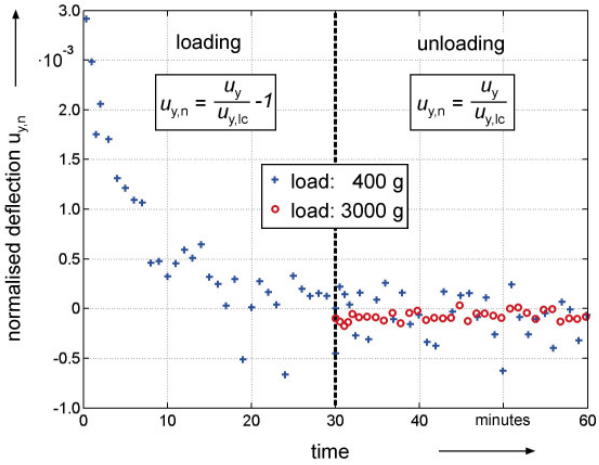

Fig. 11: Normalised deflection $u_{y,n}$ of the S-Spring as a function of the time for loading and unloading process

In order to visualise the creep behaviour the tipping corrected deflection data of the creep measurement are plotted in figure 11 as function of the time. For the loading the deflection u_y is normalised to the value $u_{y,lc}$ after load change and subtracted by 1. For the unloading the deflection is normalised to $u_{y,lc}$.

During loading for the 400 g creep measurement the deflection decreases with increasing time about $u_{y,n} = 3 \cdot 10^{-3}$. During unloading the measured deflection shows no detectable time dependence. This unexpected behaviour could not be explained by mechanical after effects of the S-Spring. In the first place mechanical after effects lead to symmetric time dependencies of the measurement signal for

loading and unloading. Secondly changes of deflection caused by mechanical after effects would lead to an increasing deflection during loading.

This behaviour could be explained by the influence of the pulley as further investigations described in [3] offered. Therefore loading creep measurements are not suitable to investigate mechanical after effects. But while unloading no force and therewith no influences of the pulley act on the S-Spring.

Due to these reasons subsequently the unloading creep measurements are used to calculate mechanical after effects of the S-Spring.

The relative mechanical after effect χ_a is defined by subtracting the deflection $u_{y,30}$ 30 minutes after load change and the deflection $u_{y,lc}$ direct after load change and relating the result to the deflection $u_{y,lc}$:

$$\chi_a = \frac{u_{y,30} - u_{y,lc}}{u_{y,lc}} \qquad (7)$$

During unloading for the 400 g measurement as well as for the 3000 g measurement no creep of the deflection data is detectable. The data seem to scatter statistical. The absolute scatter band between maximum and minimum deflection amounts 30 nm for both measurements. With this maximum value for the difference in the equation (7) the maximum relative after effect is calculated to $\chi_a = 2 \cdot 10^{-4}$.

This estimation is very conservative. The maximum and minimum value of deflection does not occur at the beginning or at the end of the creep measurement and there is no trend of the deflection values detectable. The confidence belt of the deflection values amounts 3 nm with expended uncertainty. With the value of the confidence belt for the difference in the equation (7) the relative mechanical after effect of the S-Spring results in $\chi_a = 2 \cdot 10^{-5}$. This seems to be the upper limit of the mechanical after effect bonded by the accuracy of the interferometer used for the measurement.

4.2. *Comparative investigations of silicon and metallic load cells*

To evaluate the usability of Si-LCs with thin film SGs measurements according the OIML R60 at 20°C are performed with silicon and metallic LCs.

Figure 12 shows a picture of the experimental setup used for the investigations. The fixing of the LC within the experimental setup is achieved by clamping the fixing step of the LC-body on the left side. On the right side the load force of the chain masses is introduced by dropping the masses on a piece of hardwood which lies on the body of the LC.

The loads are applied automatically by using chain masses which are dropped on the LC step by step. The seven load steps amount 0 g, 50 g, 150 g, 250 g, 450 g, 650 g and 1050 g. Every load step is applied for about one minute.

The measurements are performed on a Si-LC with thin-film SGs and three metallic-LCs of the same geometry. Two of the metallic LCs are made of stainless steel one with thin-film SGs and one with glued foil SGs. The third metallic LC is made of aluminium with glued foil SGs.

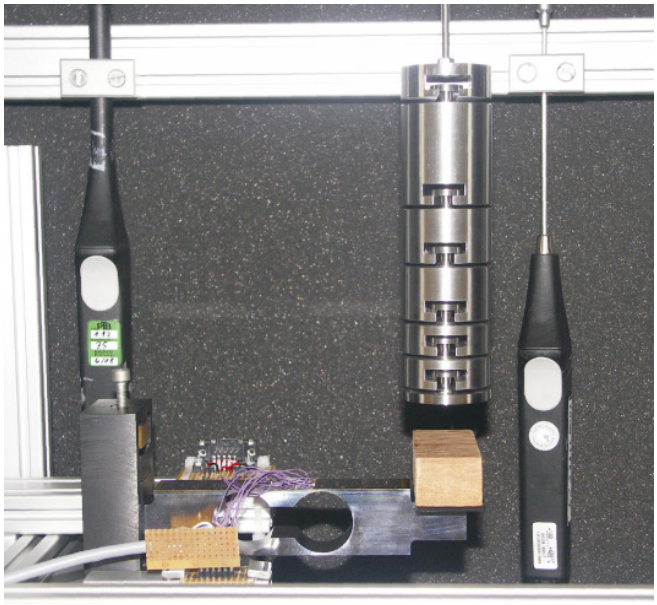

Fig. 12: The Si-LC within the experimental setup; clamped on the left side and loaded by chain masses on the right side

Subsequently two important criteria mentioned in the R60 are discussed. The load cell error E_{LC} which verifies linearity and hysteresis and the repeatability error E_{rep} which is a quantum for the reproducibility. Both the load cell error and the repeatability error have to be lower than the maximum permissible error *mpe* of the acquired accuracy class to pass the test. For all measurements an apportionment factor p_{lc} as defined in the R60 of $p_{lc} = 0.7$ is assumed.

In figure 13 the load cell error E_{LC} is plotted as function of the load (blue line) for the different LCs. Additionally the repeatability error E_{rep} is illustrated by the red marks. The *mpe* of the best class reached by the LC is limited by the black lines.

The aluminium LC with glued SGs reaches class C with 1000 verification intervals. The limiting factor is the load cell error E_{LC} caused by the hysteresis of the LC signal. Theoretically a higher class could be reached by a compensation of the hysteresis effects.

The steel LC with glued SGs attains class C with 2500 verification intervals. In contrast to the aluminium LC not the load cell error E_{LC} but the repeatability error E_{rep} is the limiting factor. This means due to the bonding reproducibility a higher class could not be reached by compensation.

The steel LC with sputtered on SGs offers a lower repeatability error E_{rep} compared to the LC with glued SGs. The LC reaches class C with 8000 verification intervals. The limiting factor is the load cell error E_{LC} caused by the hysteresis of the LC signal. Therefore a higher class could be reached by a compensation of the hysteresis effects theoretically.

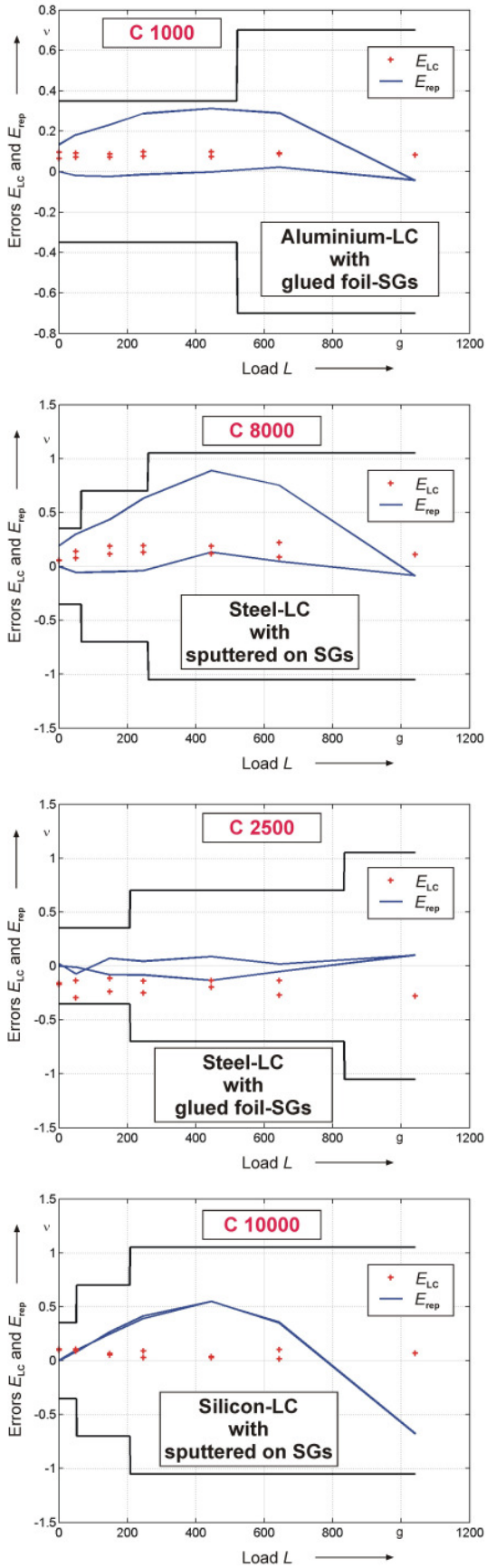

Fig. 13: Load cell error E_{LC} (blue line) and repeatability error E_{rep} (red marks) according to OIML R60 as function of the load for different LCs; additionally the maximum permissible error (black line) of the reached accuracy class is shown

The silicon LC with sputtered on SGs attains class C with 10000 verification intervals. The limiting factor is the load cell error E_{LC}. But in spite of the aluminium LC and the steel LC with sputtered on SGs this error is not caused by hysteresis. In fact the nonlinearity of the LC signal leads to the load cell error E_{LC}. That means a higher class could be reached by a compensation of the nonlinearity.

The compensation of nonlinearities is much easier than the compensation of hysteresis effects which requires models with load depending history. For the metallic LCs the compensation of nonlinearities would be no essential improvement due to the dominant influence of hysteresis effects. Therefore in the following a digital compensation of the nonlinearity is done only for the Si-LC.

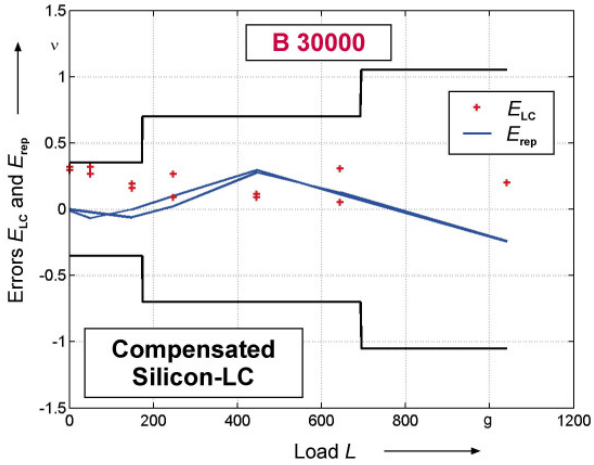

Fig. 14: Load cell error E_{LC} (blue line) and repeatability error E_{rep} (red marks) according to OIML R60 as function of the load for the Si-LC with compensated nonlinearity; Additionally the maximum permissible error (black line) is shown

Figure 14 shows the results of the silicon LC with sputtered on SGs compensated by a linear model for the nonlinearity. With this compensation the silicon LC reaches class B with 30000 verification intervals. After the compensation of the nonlinearity the limiting factor is the repeatability error E_{rep}. That means more complex compensation models with equations of higher order or models for hysteresis effects are not useful to achieve higher accuracy classes.

5. CONCLUSION

This paper presents the results of metrological investigations of load cells using crystalline materials as sensor material. Two diversity sensor systems for load cells with crystalline materials are presented and discussed.

In the first part the investigations show that piezoelectric force measurement devices in conjunction with low-drift charge amplifiers are only qualified for low-accuracy classes of load cells according to the OIML recommendation R60 (e.g. class D for ordinary-accuracy weighing instruments). Indeed the limiting factor is not, as expected, the drift. Instead, rather temperature dependencies and nonlinearities being describable through constant material coefficients are

the reason for low classification. The traceability of temperature- and linearity-effects to constant material coefficients and the high reproducibility achieved offer compensation methods, e.g., mechatronic systems known from digital load cells. Admittedly, comparable systems for piezoelectric force measurement devices are unknown up to now. But especially for high nominal loads and in conjunction with low-drift charge amplifiers, piezoelectric force measurement devices in combination with mechatronic systems seem to offer unused potential also for static precision measurements.

In the second part the experimental investigations of time depending effects of a mechanical spring made of single crystalline Si under load offer the very low time dependence of this spring. The relative mechanical after effects of the spring made of single crystalline Si are substantiated to be less than $\chi_a = 2 \cdot 10^{-5}$ and thus two orders of magnitude lower compared to metallic mechanical springs.

Load depending investigations of Si-LCs with sputtered on SGs concerning linearity, hysteresis and reproducibility at a temperature of 20°C confirm the better properties of the Si-LC compared to metallic LCs.

The classification of the LCs according to the OIML Recommendation R60 offers that the Si-LC reaches accuracy class C with 10000 verification intervals while the metallic LCs attain accuracy classes between C with 1000 verification intervals and C with 8000 verification intervals.

By a digital compensation of nonlinearities the Si-LC could attain accuracy class B with 30000 verification intervals. For the metallic LCs a compensation of the nonlinearity is not useful to achieve a higher class due to the limiting reproducibility and hysteresis effects.

The investigations point out in combination with mechatronic systems both sensor systems using crystalline materials as sensor material seem to be applicable for high precision measurements in the range of precision strain gauge load cells or even better.

REFERENCES

[1] Mack, O., "Verhalten piezoelektrischer Kraftaufnehmer unter Wirkung mechanischer Einflussgrößen", *Dissertation*, Braunschweig, 2006

[2] Mack, O., Schwartz, R., Möglichkeiten und Grenzen piezoelektrischer Kraftaufnehmer in der Kraftmess- und Wägetechnik, *47. Internationales Wissenschaftliches Kolloquium der Technischen Universität Illmenau*, 23.-26. September 2002

[3] Mäuselein, S., Mack, O., Schwartz, R., Jäger, G., "Investigations of load cells made of single-crystalline silicon with sputtered-on strain gauges", *20th TC3IMEKO International Conference*, Mexico, November 2007

[4] Baumgarten, D., "Bestimmung der elastischen Nachwirkung von Metallischen und Nichtmetallischen Federwerkstoffen im Kriechversuch", *Dissertation*, Braunschweig, 1989

[5] International Recommendation OIML R60 for load cells, Edition 2000, *Bureau International de Métrologie Légale*, Paris, France

[6] Mack, O., "Investigations of the Influence of Disturbing Components on a Piezoelectric Force Transducer", *VDI-Bericht 1685*, VDI Verlag GmbH, Düsseldorf 2002, ISBN 3-18-091685-0, pp.417-424

[7] Gautschi, G., Piezoelectric Sensorics, *Springer Verlag*, Berlin Heidelberg, 2002 ISBN 3540422595

[8] Mack, O., "Reasons for the nonlinearity of piezoelectric force transducers", *VDI-Bericht 1829*, VDI Verlag GmbH, Düsseldorf 2004, ISBN 3-18-091829-2, pp.153-161

[9] Kistler Instrumente AG, Kraft- und Drehmomentsensoren, *corporate publication No. 300-460d-09.05*

[10] Kumme, R.; Mack, O.; Bill, B.; Haab, H. R.; Gossweiler, C., "Investigation of Piezoelectric Force Measuring Devices in Force Calibration and Force Standard Machines", *Proceedings of the 17th International Conference on Force, Mass, Torque and Pressure Measurement, IMEKO TC3, 2001, Istanbul*

[11] Kumme, R.; Mack, O.; Bill, B.; Haab, H. R.; Gossweiler, C., "Dynamic Properties and Investigations of Piezoelectric Force Measuring Devices", *VDI-Bericht 1685*, VDI Verlag GmbH, Düsseldorf 2002, ISBN 3-18-091685-0, pp. 161-172

[12] Mack, O., Kumme, R., "Quasistatic and dynamic investigation methods of piezoelectric force measurement devices", *Proceedings of the IMEKO TC3/APMF, Taejon, (Republic of Korea*), 14.-18. Sept. 1998, pp.310-320

[13] Tichy, J.; Gautschi, G., "Piezoelektrische Messtechnik", *Springer Verlag*, Berlin Heidelberg, 1980 ISBN 3-540-09448-2

[14] Hruska, C., Independent verification of the values of electroelastic constants of α-quartz, *Journal of Applied Physics,* 61(3), February 1986, S. 1127-1129